Improving regular acceleration in the nonlinear interaction of particles and waves

R. Pakter and G. Corso

Citation: Physics of Plasmas **2**, 4312 (1995); doi: 10.1063/1.870986
View online: http://dx.doi.org/10.1063/1.870986
View Table of Contents: http://scitation.aip.org/content/aip/journal/pop/2/11?ver=pdfcov
Published by the AIP Publishing

Improving regular acceleration in the nonlinear interaction of particles and waves

R. Pakter and G. Corso
Instituto de Física–Universidade Federal do Rio Grande do Sul, Caixa Postal 15051, 91501-970 Porto Alegre, RS, Brazil

(Received 13 February 1995; accepted 27 July 1995)

In this work one studies the effects arising from the inclusion of a stationary extraordinary mode in the resonant interaction of magnetized particles and perpendicularly propagating electrostatic waves. It is found that for a stationary mode frequency of the order of the Larmor frequency and with a suitably chosen amplitude, one is able to suppress the resonance which drives the weakly relativistic dynamics into chaos. Improved regular acceleration of initially low energy particles is thus attained. Analytical estimates of the optimal stationary mode amplitude is presented. A detailed study of the topological effects due to resonance suppression based on bifurcation analysis is performed. The main results are verified with the help of single particle numerical simulations.

I. INTRODUCTION

With the advent of powerful radiation-generation systems such as free-electron lasers, cyclotrons autoresonance masers, gyrotrons and ion-channel lasers, a good deal of effort has been directed to the study of the interaction of low energy particles and large-amplitude waves.[1–8] Whenever wave-particle exchange is likely to occur, particles can be highly accelerated, which is of importance in particle acceleration and in current drive techniques of controlled thermonuclear research.

Theoretical models have been developed to investigate the interaction of magnetized particles and strong perpendicular waves in cyclotronic systems.[6–10] In particular, Davidson *et al.*[6] have shown that the nonlinear electron dynamics plays an important role in wave-particle coupling. They investigated the regular interaction of weakly relativistic particles and ordinarily polarized electromagnetic waves. Relativistic mass variation detunes the initially resonant interaction, saturating the energy exchange. The maximum action excursion was found to scale with the wave amplitude A_w as $A_w^{2/3}$.

On the other hand, Corso and Rizzato[7] have performed an analysis based on a Hamiltonian formalism of the regular and stochastic dynamics that takes place in a low energy cyclotron system as it is perturbed by a perpendicular propagating electrostatic wave. They have found that even for *small* wave amplitudes the low energy electron motion may become chaotic, with a subsequent stochastic diffusion of the particle beam. They also found that an effective regular particle acceleration seems to be possible only deep inside the weakly relativistic region.

In the Hamiltonian framework the onset of chaos and stochastic diffusion can be well understood following the Chirikov scenario.[11,12] Near each of the wave-particle resonances, there appear Kolmogorov-Arnold-Moser (KAM) surfaces isolating groups of pendulum-like islands surrounded by thin stochastic layers. As the wave amplitude increases, the islands grow until different groups touch each other, destroying KAM surfaces and causing particles to stochastically diffuse throughout the phase space. Although the above scenario is fairly general, it is not typical of the low energy case where the dynamics is dictated by relativistic effects and where the major resonance island presents nonpendulum behavior. In this case, no homoclinic chaos develops along the island boundary since the boundary has a finite rotating frequency.[13] The onset of chaos for weakly relativistic particles is mainly due to resonance overlap with the adjacent pendulum-like island.

Keeping all this information in perspective, in this paper we will study how one can interfere with the wave-particle interaction in order to avoid a premature overlap of the low energy island with its adjacent one. If this program can be accomplished, the phase space may be regularized, which would result in a higher acceleration of particles. We will analyze the effects due to the introduction of a stationary extraordinary mode in the resonant dynamics of a cyclotronic system perturbed by transversal electrostatic waves. The main idea will be to generate, by means of the stationary mode, a resonance that destructively interferes with the wave-particle resonance, thereby regularizing the *low energy* region of phase-space. It will be shown that for a judicious choice of the stationary mode amplitude the dynamics of initially low energy particles can undergo strong modifications, varying from completely diffuse to regular with highly increased acceleration. Numerical results obtained by direct integration of the equations of motion will be shown in order to test the validity of the method.

II. MODEL

Consider a relativistic electron beam immersed in a low density, cold, magnetized plasma, with background magnetic field given by $\mathbf{B}_0 = B_0\hat{z}$, perturbed both by a transversal electrostatic wave and a stationary extraordinary mode. The vector potential related to $\mathbf{B}_0$ is written as $\mathbf{A}_0 = B_0 x\hat{y}$.

 1070-664X/95/2(11)/4312/13/$6.00

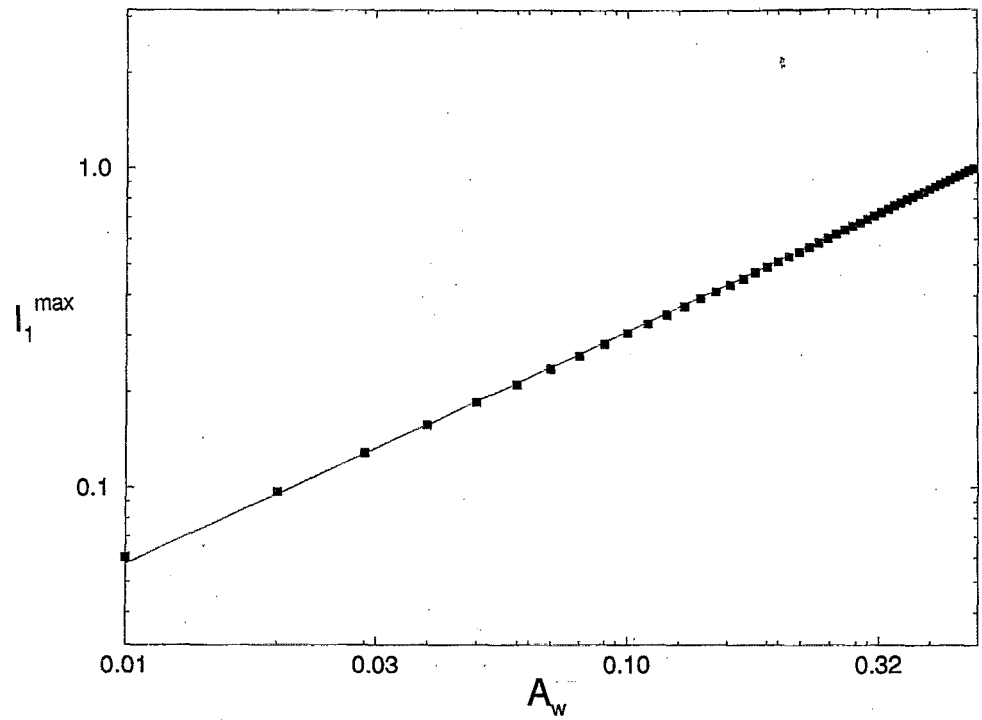

FIG. 1. Maximum action excursion I_{max} vs. the wave amplitude A_w for $k=1$ in a log-log graphic. Squares represent values calculated from Eq. (7). The solid line is obtained by linear regression. The scaling exponent is found to be $\alpha=0.73$.

The electrostatic wave has an amplitude A_w and propagates in the x-direction with wave vector k and frequency ω_h. It is assumed to be a magnetized Langmuir wave with Debye length sufficiently small that one can consider the frequency to be independent of the wave vector. Assuming $\omega_p \ll \omega_{c0}$, we have for the wave frequency $\omega_h^2=\omega_{c0}^2+\omega_p^2\approx\omega_{c0}^2$, with ω_p as the plasma frequency and $\omega_{c0}\equiv|e|\times B_0/mc$ as the nonrelativistic electron cyclotron frequency.

The stationary extraordinary mode has frequency ω_X and wave vector $k_X\hat{x}$ related to each other by the cold dispersion relation. The following expression for the extraordinary mode vector potential is assumed:

$$\frac{e\mathbf{A}_X}{mc^2}=\varepsilon'[\eta_x \sin(k_Xx)\sin(\omega_Xt)\hat{x} + \eta_y \sin(k_Xx)\cos(\omega_Xt)\hat{y}],$$

where $\varepsilon'=E/\omega_X$ is the mode amplitude, with E the electric field amplitude, and η_x and η_y are the components of the polarization vector. Let us choose the frequency in order to satisfy the following relation, $\omega_X^2-\omega_h^2\approx\omega_p^2$, such that it is near the right-hand cut-off frequency. If this is the case, the mode is approximately circularly polarized with $\eta_y=-\eta_x=1$, and the relation $ck_X/\omega_X\approx\omega_p/\omega_{c0}\ll 1$ is valid. Taking into account the above relation and the fact that we will be interested in the low energy particles we can safely assume $k_Xr_L\ll 1$ (with r_L as the particle Larmor radius), which enables one to write $\mathbf{A}\equiv\mathbf{A}_0+\mathbf{A}_X$ as

$$\frac{e\mathbf{A}}{mc^2}=B_0x\{-\varepsilon \sin(\omega_Xt)\hat{x}+[1+\varepsilon \cos(\omega_Xt)]\hat{y}\},$$

where $\varepsilon\equiv k_X\varepsilon'/B_0$.

Scaling time and distance to ω_{c0} and ω_{c0}/c, the dimensionless particle Hamiltonian is given by

$$H=\sqrt{1+[P_x-\varepsilon x \sin(\omega_Xt)]^2+\{P_y+x[1+\varepsilon \cos(\omega_Xt)]\}^2+P_z^2}+A_w \cos(kx-\omega_ht), \quad (1)$$

where energy, momentum, potential vector and scalar potential are normalized to mc^2, mc, mc^2/e and e/mc^2, respectively. It is readily seen from the Hamiltonian that P_y and P_z are constants of motion. As we are considering particles with very low initial energies, we will set $P_z=0$ and, for simplicity, $P_y=0$. Introducing canonical guiding-center variables, I and θ, related to Cartesian coordinates through

$$P_x=\sqrt{2I}\cos\theta,$$

$$x=\sqrt{2I}\sin\theta,$$

and using the harmonic expansion for Bessel functions, it is possible to write the Hamiltonian in the form

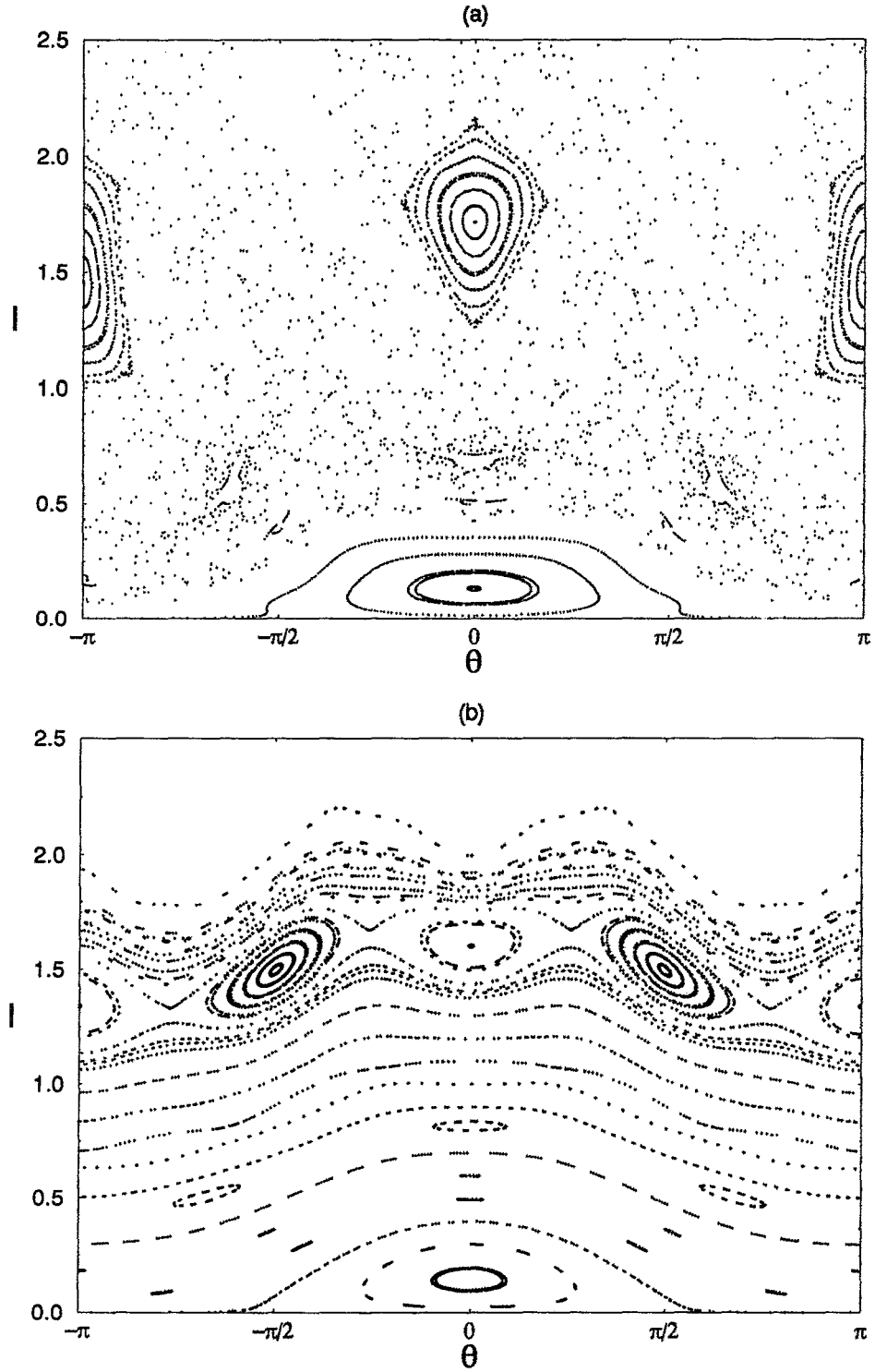

FIG. 2. Poincaré plot for $A_w=0.12$ and $k=1$ with $\varepsilon=0$ (a) and $\varepsilon=\varepsilon_{op}=4.632\times10^{-2}$ (b).

$$H=\sqrt{1+2I+4\varepsilon I[\sin^2\theta\cos(\omega_X t)-\cos\theta\sin\theta\sin(\omega_X t)]}+A_w\sum_{n=-\infty}^{+\infty}J_n(k\sqrt{2I})\cos(n\theta-\omega_h t), \quad (2)$$

where the term proportional to ε^2 is discarded. For the unperturbed system ($A_w=\varepsilon=0$), θ represents the electron gyromotion phase, and I the transversal energy $p_\perp^2/2$. Since the differences between the frequencies involved in the above system, ω_{c0}, ω_X and ω_h, are all of the order of $\omega_p^2\ll1$, it will be assumed in the following that $\omega_h=\omega_X=\omega_{c0}$ (or in adimensional form $\omega_h=\omega_X=1$).

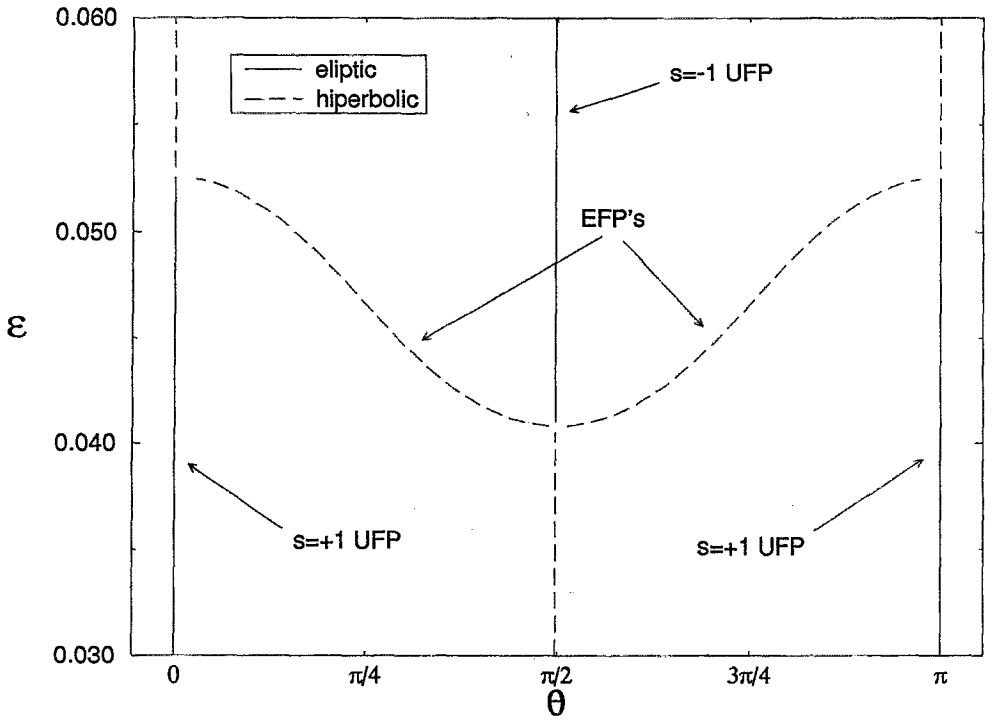

FIG. 3. Fixed point dynamics as ε is varied. Parameters are the same as in Fig. 2. The resonance suppression region is represented by the interval of EFP's existence.

III. ANALYSIS OF THE RESONANCES

In this section we analyze the resonances in the particle motion described by the Hamiltonian (2) derived above. In order to make the analysis clearer we will study separately the pendulum-like and non-pendulum-like wave-particle resonances caused by the electrostatic wave and the stationary mode.

A. Pendulum-like electrostatic wave-particle resonances

Let us by now focus on the perturbations of the particle motion due to the electrostatic wave. The appearance of primary wave-particle resonances is related to each of the harmonics in the last term of the Hamiltonian (2). Their location in phase space can be estimated from $d_t(n\theta - t) \sim 0$. This leads to an approximate expression, valid to zero order, for the action at the nth resonance

$$I_n = \frac{n^2 - 1}{2}, \quad n \geq 2. \tag{3}$$

For $n=1$ the above relation is no longer valid because for small I, terms proportional to A_w cannot be disregarded in $d_t\theta$,[7,8] leading to several changes in the particles motion. This case will be treated in detail in the next sub-section.

Assuming that the particle trajectory is near to a given resonance and that the wave amplitude is *small* enough that contributions of other harmonics can be safely disregarded, the action can be expanded around I_n and one is able to approximate the Hamiltonian expression (2) by a pendulum-like one

$$h^{(n)}(\hat{I}, \theta) = (G/2)\hat{I}^2 - F\cos(n\theta), \tag{4}$$

where $\hat{I} \equiv I - I_n$, $G = -(1+2I_n)^{3/2} = -1/n^3$ and $F = -A_w J_n(k\sqrt{2I_n})$, and a time-removal canonical transformation—$n\theta - t \to n\theta$, $I \to I$ and $H \to h^{(n)} = H - I/n$—has been performed. Analyzing the fixed points in the dynamics of the above Hamiltonian we find n hyperbolic points and n elliptic points appearing for $n\theta = 2m\pi$, with $m \leq n$ an integer. The character of the points depends on the signal of F.

We can also calculate the maximum action excursion around I_n for particles trapped in the pendulum-like resonant island. This quantity, which will be called $\Delta I_n^{pend} \equiv I_{max} - I_n$, is relevant in island overlap calculations and is found to be

$$\Delta I_n^{pend} = 2\sqrt{F/G} = 2\sqrt{n^3 A_w J_n(k\sqrt{2I_n})}. \tag{5}$$

As expected, the maximum action excursion scales as $A_w^{1/2}$.

B. Non-pendulum-like electrostatic wave-particle resonance

As quoted before, in the low energy case we cannot neglect wave terms even in zeroth order calculation and particle trajectories significantly differ from a pendular one. To see this we analyze the Hamiltonian (2) disregarding the extraordinary mode and taking into account the leading contributions for $I \lesssim 1$. The important term in the summation (2) is the one with $n=1$. Performing a time-removal canonical transformation—$\theta - t \to \theta$, $I \to I$ and $H \to h^{(1)} = H - I$—the Hamiltonian assumes the form

$$h^{(1)}(I, \theta) = \sqrt{1+2I} - I + A_w J_1(k\sqrt{2I})\cos\theta. \tag{6}$$

This Hamiltonian has been extensively studied in the limit

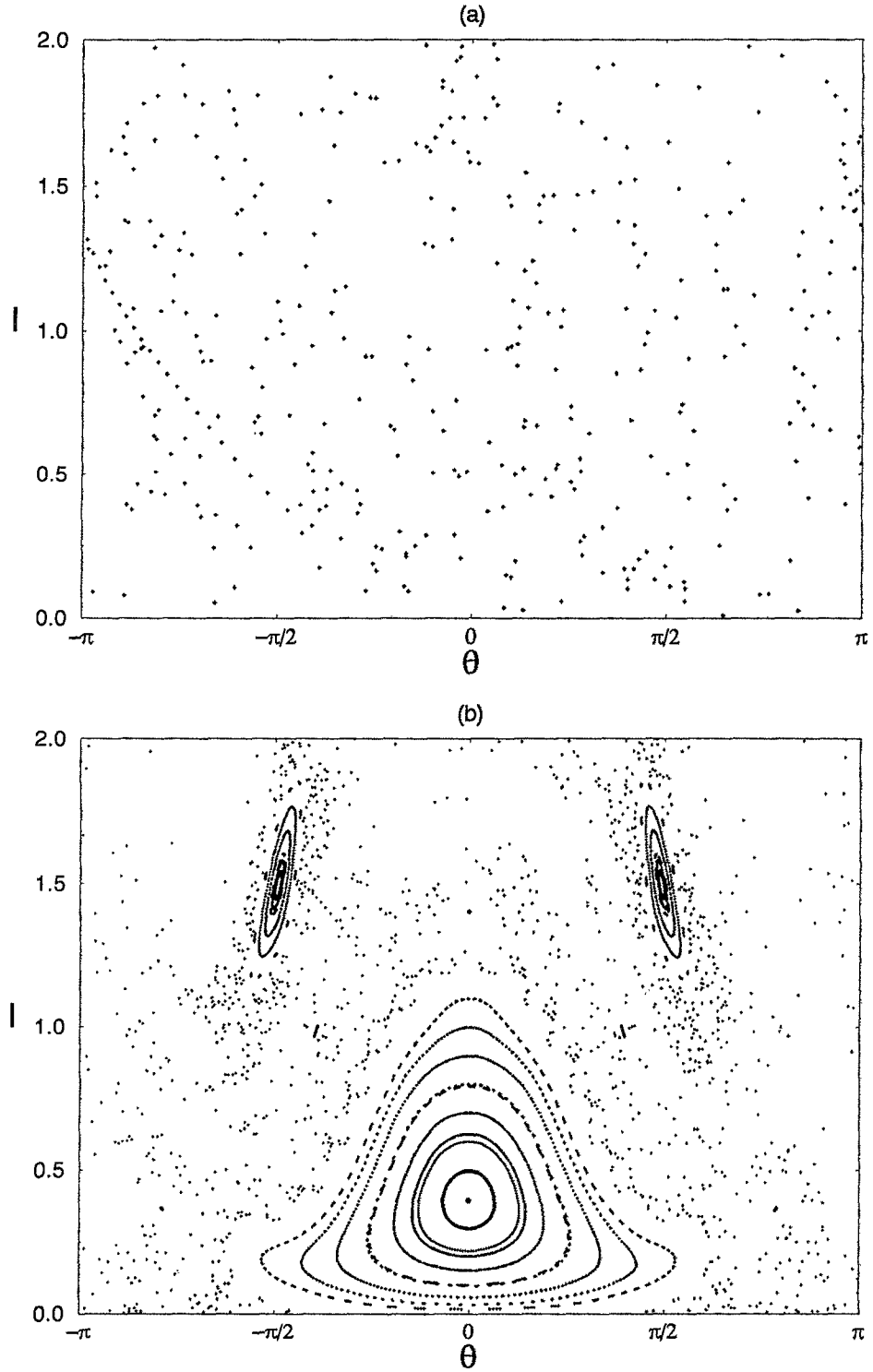

FIG. 4. Poincaré plot for $A_w=0.4$ and $k=1$ with $\varepsilon=0$ (a) and $\varepsilon=\varepsilon_{op}=1.544\times10^{-1}$ (b).

$I\ll1$ in Ref. 13. Trajectories described by (6) may be either trapped or untrapped. Trapped ones present a triangular shape instead of the typical pendulum-like one.

Particles that initially have very low energies ($I\approx0$) will evolve in time along the boundary which separates trapped and untrapped trajectories. Analyzing their dynamics one concludes that during the very beginning of motion these particles will rapidly migrate to $\theta=\pi/2$ generating a bunch there. This happens because of the term proportional to $\cos\theta/\sqrt{I}$ that appears in the equation $d_t\theta=\partial h^{(1)}/\partial\hat{I}$. The

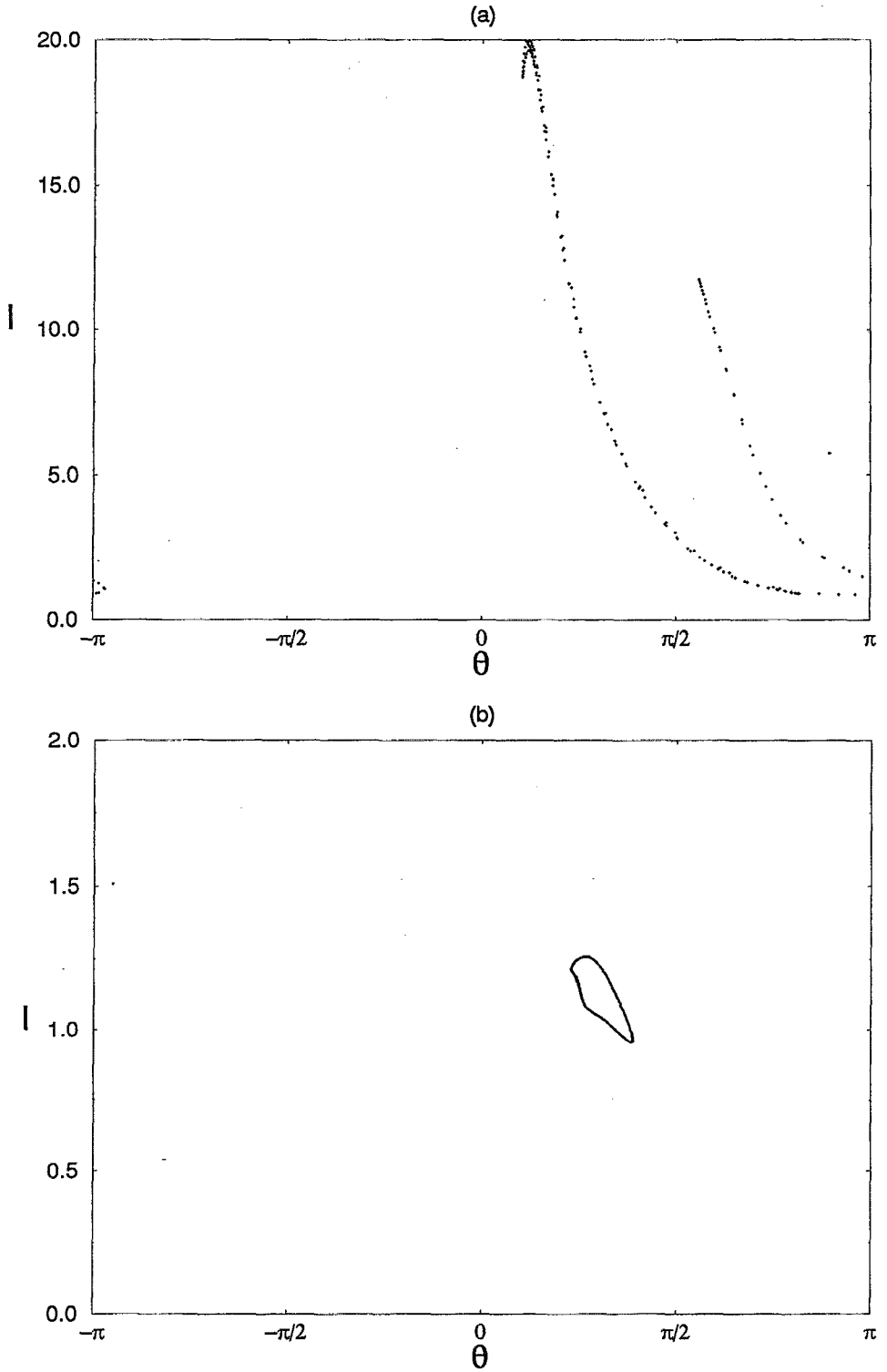

FIG. 5. Phase space of 200 initially low energy particles after 45 wave periods for $A_w=0.4$ and $k=1$. In (a) $\varepsilon=0$ and in (b) $\varepsilon=\varepsilon_{op}=1.544\times10^{-1}$. Initial conditions are $I=10^{-2}$ and phases homogeneously distributed over $0<\theta<2\pi$.

value of the Hamiltonian along the boundary is $h^{(1)}(I,\theta)=1$, so the maximum action excursion, I_1^{max}, for these particles can be calculated by the following equation

$$\sqrt{1+2I_1^{max}}-I_1^{max}+A_wJ_1(k\sqrt{2I_1^{max}})=1, \tag{7}$$

which gives the maximum I value on the boundary.

In Fig. 1 I_1^{max} vs. the wave amplitude A_w for $k=1$ is presented in a log-log graphic. The value of k was chosen in order to have a dynamics of the relativistic type, which means that the agent responsible for the nonpendulum island saturation is in fact the relativistic mass variation (the nonlinear term $\sqrt{1+2I}$ in the Hamiltonian) and not the roots of

$J_1(k\sqrt{2I})$.[7] From the figure it can be verified that even for not so small amplitudes I_1^{max} scales with A_w as $I_1^{max} \sim A_w^{\alpha}$. The value of α was found to be approximately given by $\alpha = 0.73$. This value seems to depend only slightly on k, since we are deep inside the relativistic regime.

The analysis made in the previous paragraph is, of course, of no physical meaning if we are dealing only with the electrostatic wave perturbation. This is so because even for *small* values of A_w the overlap between the first $(n=1)$ and the second $(n=2)$ resonant islands is likely to occur, invalidating the above analysis. In fact, a condition for resonance overlapping concerning these islands is written as

$$I_1^{max} + \Delta I_2^{pend} = I_2 . \tag{8}$$

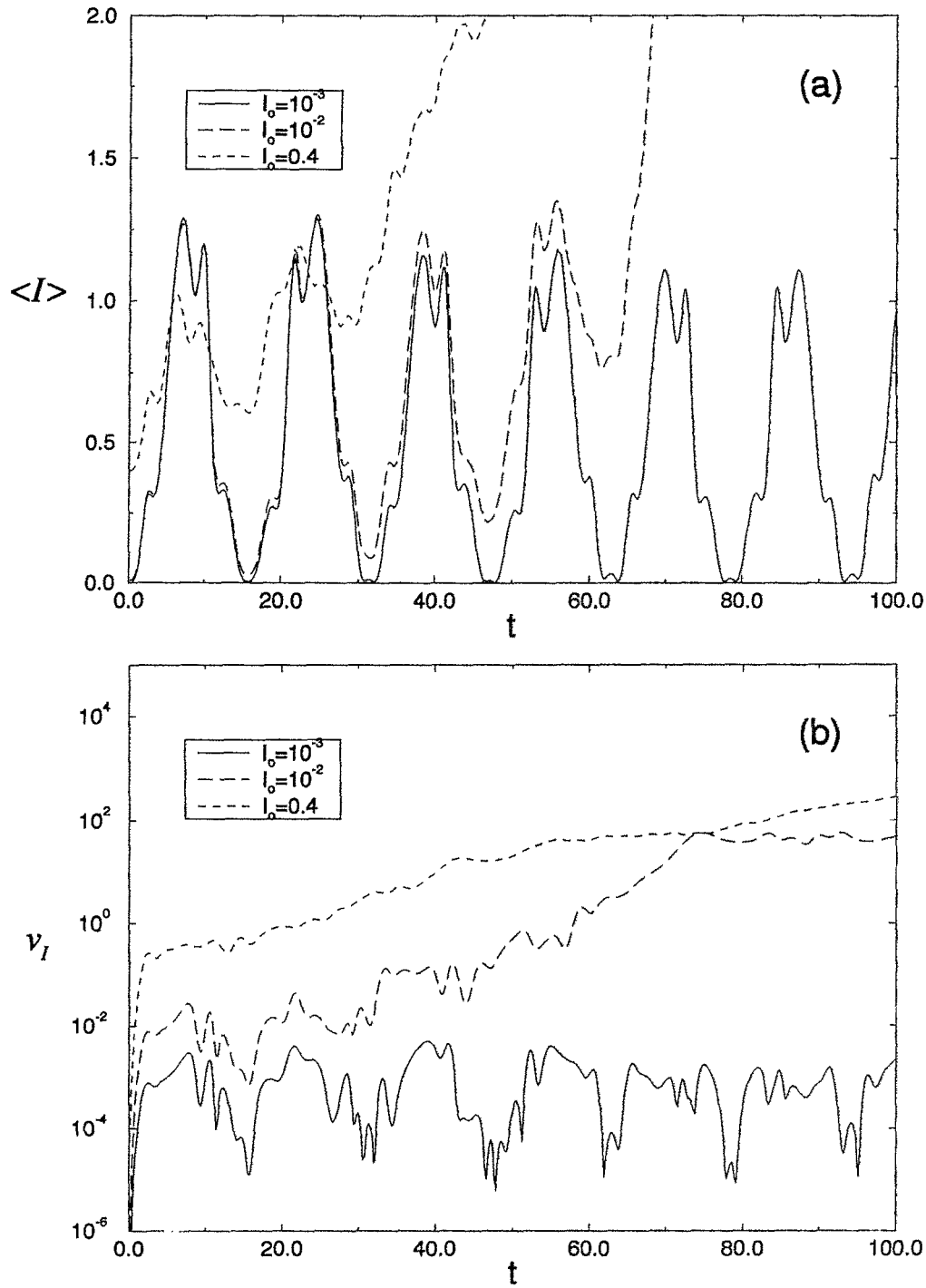

FIG. 6. Bunching dynamics of 250 particles as initial action value I_o is varied for a fixed $A_w = 0.5$. Solid lines correspond to $I_o = 10^{-3}$, long dashed lines to $I_o = 10^{-2}$ and dashed lines to $I_o = 4 \times 10^{-1}$. Graphics (a), (b) and (c) show the time evolution of the mean action $\langle I \rangle$, the action variance $\nu_I \equiv \langle I^2 \rangle - \langle I \rangle^2$ and the bunching parameter modulus $|b| \equiv |\langle e^{i\theta} \rangle|$, respectively.

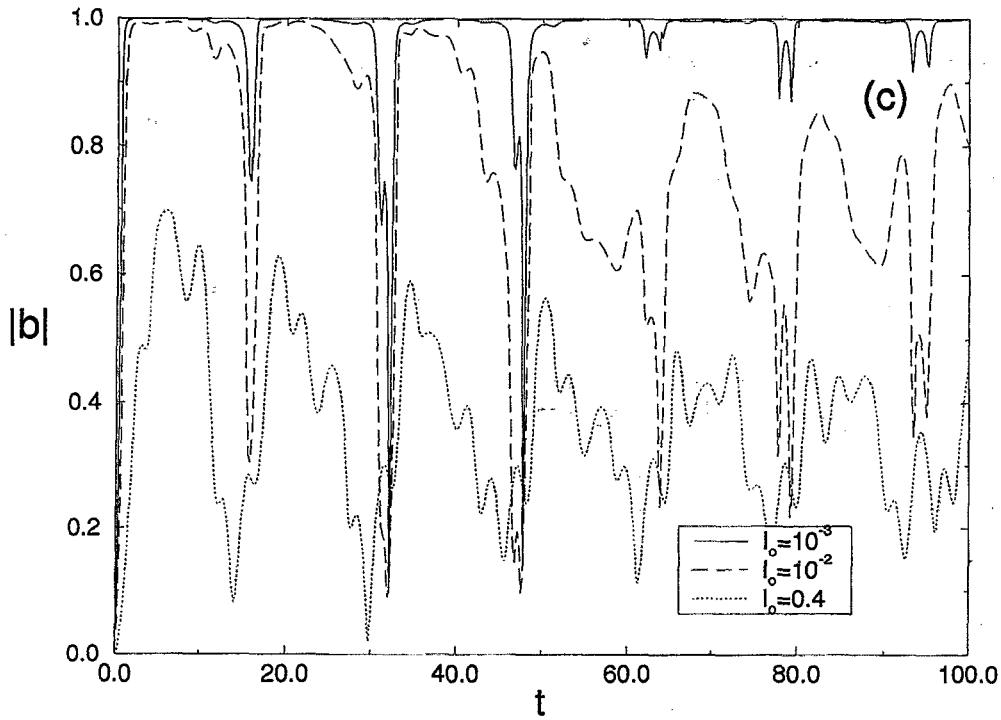

FIG. 6. (*Continued.*)

Isolating I_1^{max} as a function of A_w in the above expression and using it in Eq. (7), we find a closed equation for the wave amplitude threshold, $A_{w,th}$, above which resonance overlapping between the first and second islands occurs. For $k=1$ we find $A_{w,th}=0.135$. As expected, the analysis does not seem to be valid. However, as will be shown in Sec. IV, the introduction of a stationary extraordinary mode reduces second island amplitude, preventing the premature overlap and improving the regular energization of particles.

C. Stationary mode-particle resonances

In order to study the resonances caused by the stationary mode, let us take $A_w=0$ and expand the Hamiltonian (2) for small ε. Considering only first order terms, we have

$$H=\sqrt{1+2I}+\frac{\varepsilon I}{\sqrt{1+2I}}[\cos t-\cos(2\theta-t)]. \tag{9}$$

The only perturbing term that resonantly interacts with the particles is the one containing the harmonic $2\theta-t$. The other has no expressive influence in any part of the phase space.

The stationary wave-particle resonance thus appears for $d_t\theta\sim 1/2$ and is a pendulum-like one, with $G=-1/2^3$ and $F=\varepsilon I_2/\sqrt{1+2I_2}$ in Eq. (4). The same considerations presented in Sec. III-A concerning pendulum-like resonances, with $n=2$, are applicable in this case and will not be discussed again.

IV. RESONANCE SUPPRESSION

From what has been discussed, we see that what is mainly responsible for the chaotization of low energy dynamics is the overlap of the $n=2$ electrostatic wave resonance with the $n=1$ nonpendulum resonance. Moreover, we see that the main contribution of the stationary mode occurs at the same location of the phase-space as the one occupied by the second resonance. So, in this section, we will analyze how we can use the stationary wave-particle resonance to destructively interfere with the second electrostatic wave-particle resonance and find the effects of this resonance suppression.

Let us begin by analyzing the optimal stationary mode amplitude, ε_{op}, in order to suppress the second electrostatic wave-particle resonance. Comparing the perturbation amplitudes of the electrostatic wave, Eq. (4), and the stationary mode, Eq. (9), for $I=I_2$, we can obtain an approximate value for ε_{op} as

$$\varepsilon_{op}=\frac{A_w\sqrt{1+2I_2}}{I_2}J_2(k\sqrt{2I_2}). \tag{10}$$

Although at first glance the resonance suppression, as it is presented here, seems to lead to a complete cut out of the resonance, it actually leads to much more involved effects to be discussed next.

To better understand the effects of the resonance suppression, one can analyze the dynamics of the particles near the second resonance by studying the *dynamics of the fixed points* of the island as ε is varied. In order to do so, let one rewrite the pendulum-like Hamiltonian (4), now taking into account the influence of the stationary mode and also keeping linear terms of $\hat{I}=I-I_2$ in the perturbation. The importance of the inclusion of linear terms in $\hat{I}$ will be apparent. The Hamiltonian takes the form

$$h^{(2)}(\hat{I},\theta)=(G/2)\hat{I}^2$$

$$+[A_w(\alpha_0+\alpha_1\hat{I})-\varepsilon(\beta_0+\beta_1\hat{I})]\cos(2\theta), \qquad (11)$$

where α_i and β_i are the coefficients of the Taylor expansion, around I_2, of $J_2(k\sqrt{2I})$ and of $I/\sqrt{1+2I}$, respectively. The equations of motion are given by

$$d_t\hat{I}=2[A_w(\alpha_0+\alpha_1\hat{I})-\varepsilon(\beta_0+\beta_1\hat{I})]\sin(2\theta)$$

and

$$d_t\theta=G\hat{I}+(A_w\alpha_1-\varepsilon\beta_1)\cos(2\theta).$$

The fixed points are those which satisfy $d_t\theta=d_t\hat{I}=0$.

Usual fixed points. From the above equations, one concludes that, similar to the case $\varepsilon=0$, usual pendulum-like

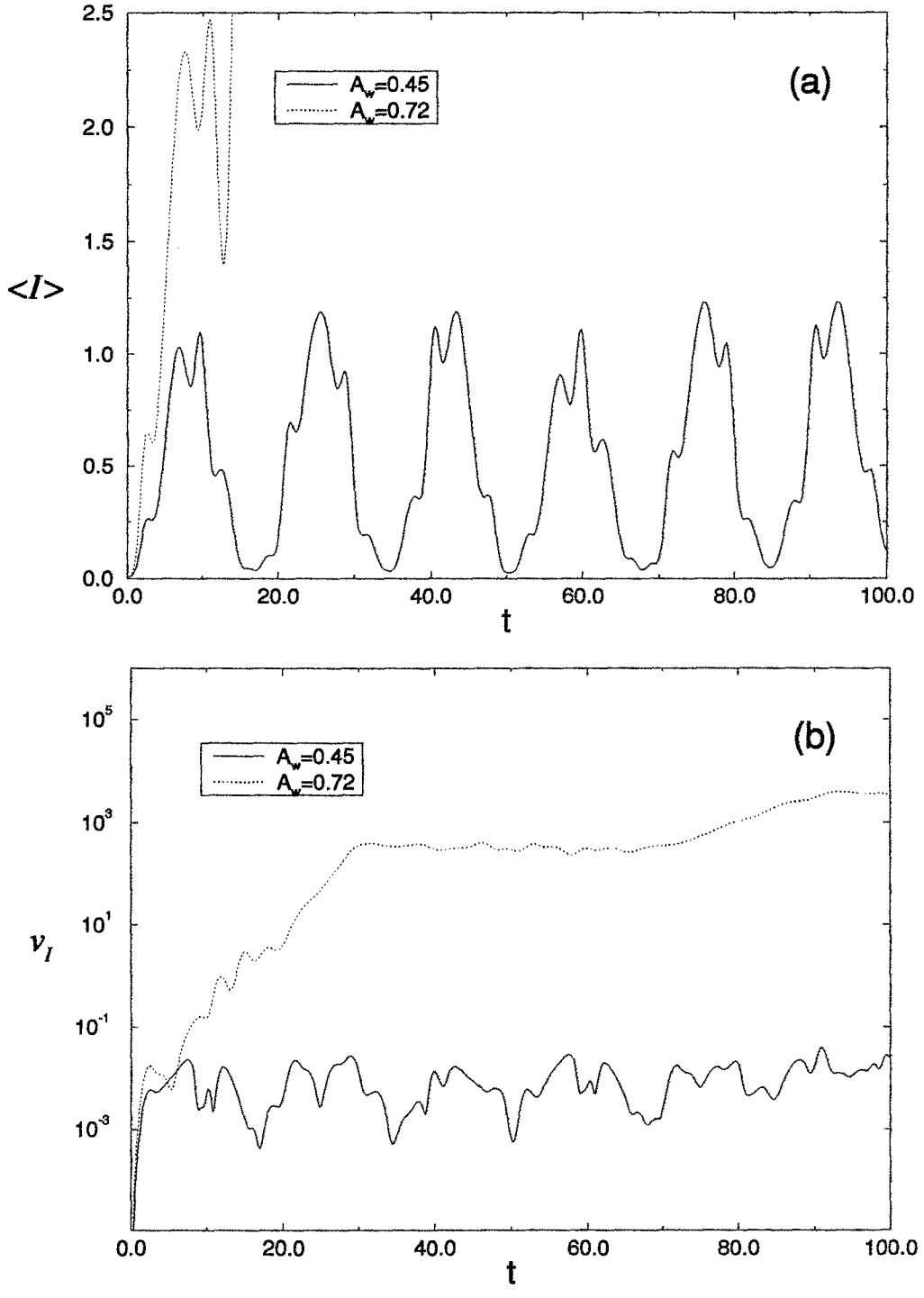

FIG. 7. Bunching dynamics of 250 particles as wave amplitude A_w is varied for a fixed $I_o=10^{-2}$. Solid lines correspond to $A_w=0.45$ and dashed lines to $A_w=0.72$. Graphics (a), (b) and (c) show the time evolution of the mean action $\langle I\rangle$, the action variance $v_I\equiv\langle I^2\rangle-\langle I\rangle^2$ and the bunching parameter *modulus* $|b|\equiv|\langle e^{i\theta}\rangle|$, respectively.

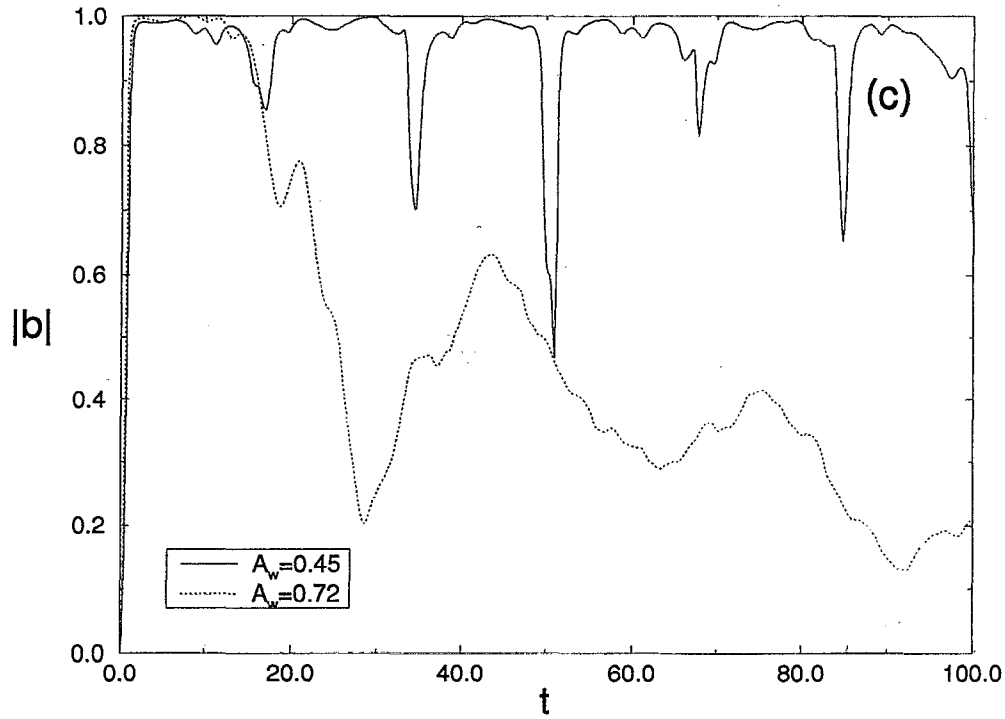

FIG. 7. (*Continued.*)

fixed points (UFP) appear for $2\theta_{UFP}=m\pi$ and $\hat{I}_{UFP}=-s(A_w\alpha_1-\varepsilon\beta_1)/G$, where $m=1,2$ and $s=\cos(m\pi)=\pm 1$. In order to analyze their stability, one calculates the matrix eigenvalues λ_{UFP} of the linearized motion around the UFP's. If the eigenvalues are real the surrounding orbits have an expanding direction and a contracting direction, thus the UFP is hyperbolic. Otherwise, the surrounding orbits circulate around the UFP which is therefore elliptic. It is found that

$$\lambda_{UFP}=\pm 2\sqrt{G(A_w\alpha_0-\varepsilon\beta_0)s-(A_w\alpha_1-\varepsilon\beta_1)^2}. \quad (12)$$

Unless the stationary mode amplitude is near the optimal one (which means $A_w\alpha_0\approx\varepsilon\beta_0$) the leading term in the square root is the leftmost one. So, as in the pendulum case, the stability of the UFP's is governed by the value of s and half of them are hyperbolic, half are elliptic. For ε small compared to A_w the elliptic ones are those for which $s=+1$, otherwise the $s=-1$ are stable.

If, on the other hand, ε is near its optimal value, such that the condition

$$|A_w\alpha_0-\varepsilon\beta_0|<\left|\frac{(A_w\alpha_1-\varepsilon\beta_1)^2}{G}\right| \quad (13)$$

is satisfied, λ_{UFP} is always imaginary and all the UFP's are of the elliptic type irrespective of s value.

Extra fixed points. A more detailed inspection of the equations of motion for $\hat{I}$ and θ, reveals that an extra set of fixed points, which shall be called EFP, may appear. If the condition (13) holds, a different set of real roots of the motion equations are found for $\hat{I}_{EFP}=-(A_w\alpha_0-\varepsilon\beta_0)/(A_w\alpha_1-\varepsilon\beta_1)$ and $2\theta_{EFP}=\cos^{-1}[G(A_w\alpha_0-\varepsilon\beta_0)/(A_w\alpha_1-\varepsilon\beta_1)^2]$. For increasing ε these points are initially located at the same position occupied by the unstable $s=-1$ UFP. Then they start migrating in the direction of the $s=+1$ UFP, colliding with them and being extinguished. Analyzing the EFP stability one finds that the matrix eigenvalues λ_{EFP} are always real during the *existence* interval of the fixed points.

The dynamics of the fixed points can be summarized as follows. As one varies ε from very small to very high values compared to A_w the UFP's initially present a typical pendulum-like behavior where the $s=+1$ points are stable and the $s=-1$ ones are unstable. During the *resonance suppression*, the unstable UFP's go stable, originating the unstable EFP's (note that at this moment all UFP are stable). The latter then travel in the direction of the $s=+1$ UFP's, colliding with them and being extinguished. In the collision, the $s=+1$ UFP's become unstable and the scenario turns back to the pendulum one, now with exchanged elliptic and hyperbolic points. Thus, by suppressing a resonance one is not simply turning off a resonance. On the contrary, one is stabilizing all major pendulum-like fixed points of the chosen resonant island, interfering in the mechanism of homoclinic intersection and leading to a suppression of chaos in the neighborhood.

Let us now estimate the maximum value of the wave amplitude, A_w^{max}, above which we can no longer attain regular acceleration even for optimal stationary mode amplitude. During the resonance suppression the second island does not completely disappear (it just changes its shape), so we can estimate the maximum $\hat{I}$ excursion for a trapped particle, ΔI_2^{sup}. When we have $\varepsilon=\varepsilon_{op}$, terms independent of $\hat{I}$ in Hamiltonian (11) cancel each other ($A_w\alpha_0=\varepsilon_{op}\beta_0$) and the equation of the boundary is $\hat{I}=2(A_w\alpha_1-\varepsilon_{op}\beta_1)\cos(2\theta)/G$ and $\hat{I}=0$. Thus, the maximum excursion is given by

$$\Delta I_2^{sup}=\left|\frac{2(A_w\alpha_1-\varepsilon_{op}\beta_1)}{G}\right|$$

$$=16A_w\left\{\frac{k}{2\sqrt{2I_2}}[J_1-J_3]-\frac{J_2}{I_2}\left[1-\frac{I_2}{(1+2I_2)}\right]\right\}, \quad (14)$$

where Eq. (10) has been used and the argument of the Bessel functions J_i is $k\sqrt{2I_2}$. Using ΔI_2^{sup} instead of ΔI_2^{pend} in the overlapping condition Eq. (8), isolating I_{max} and using the result in Eq. (7) we find a closed formula to compute A_w^{max}. For $k=1$ it is readily found $A_w^{max}=0.68$, which leads to an energy $\gamma\sim 1.8$, with γ as the relativistic factor.

V. NUMERICAL VERIFICATIONS

Up to the present point, we have made a number of analytical estimates concerning the global behavior of the system we are studying. Now, we will verify the accuracy of our analytical estimates with a series of numerical integrations of the particle orbits.

Let us begin by analyzing the behavior of the second island as we introduce the stationary extraordinary mode. In order to do so we study a small amplitude case, where the structure of the islands is not too deformed. In Fig. 2, the Poincaré plots of the *same* system are compared without [Fig. 2(a)] and with [Fig. 2(b)] the stationary mode for $A_w=0.12$. It is readily seen from Fig. 2(b), where $\varepsilon=\varepsilon_{op}=4.632\times 10^{-2}$, the efficiency of chaos suppression in the low energy part of phase-space.

It should also be noted in Fig. 2(b) the presence of the EFP's and the fact that all the UFP's appearing for $\theta=(m\pi)/2$, whatever the value of m, are elliptic points. The dynamics of the fixed points is shown in more detail in Fig. 3. By means of a Newton-Raphson algorithm[14,15] the dynamical periodic orbits (fixed points in the Poincaré plot) are followed and their linear stability determined as one varies ε. Stable periodic orbits are represented by solid lines, while unstable ones by dotted lines. One can notice a great agreement between the fixed point dynamics presented in this figure and that described in Sec. IV. The resonance suppression interval (the interval of existence of the EFP's) is approximately $\varepsilon\in[0.041,0.053]$ which is in good agreement with the predicted optimal value.

Now let us turn to the case of higher wave amplitude, where large acceleration of initially low energy particles is expected to occur. In Fig. 4, the Poincaré plots of a system are again compared without [Fig. 4(a)] and with [Fig. 4(b)] the stationary mode. Now the amplitude is $A_w=0.4$. For $\varepsilon=0$ [Fig. 4(a)] a completely chaotic phase-space is presented. All major stable fixed points of both the first and second resonant islands have already undergone infinite cascades of periodic doubling and are not present. In fact, no structure is apparent anymore. One can expect some relatively fast particle diffusion for this deep stochastic regime.

On the other hand, in Fig. 4(b), when the stationary mode is turned on with an optimal amplitude $\varepsilon=\varepsilon_{op}=1.544\times 10^{-1}$ the Poincaré plot is dramatically changed. Some stable fixed points of the first two islands are again present. The whole structure of the first nonpendulum island is restored, which leads to high regular acceleration of initially low energy particles.

In order to verify the bunching effect and the acceleration that takes place, in Fig. 5 the phase space of 200 particles after a time $t=45$ is shown. Particles initially have low energies ($I_o\equiv I(t=0)=10^{-2}$) and are uniformly distributed over $0<\theta<2\pi$. In Fig. 5(a), $\varepsilon=0$. A stochastic heating with spreading of the beam occurs in this case. For $\varepsilon=\varepsilon_{op}$, Fig. 5(b), the presence of a bunch with $I_{max}\approx 1.1$ is found. This acceleration corresponds to an energy $\gamma\approx 1.78$.

From all comparisons made up to the moment, one may be already convinced of the acceleration improvement obtained as the stationary extraordinary mode with an amplitude ε_{op} is introduced. Thus, from now on we will focus on the analysis of the bunch dynamics that takes place for $\varepsilon=\varepsilon_{op}$ calculated from Eq. (10). In order to perform this analysis, we integrate the trajectory of 250 particles that initially have the same action value I_o and are uniformly distributed over $0<\theta<2\pi$ and compute the average action value $\langle I\rangle$, the action variance $v_I\equiv\langle I^2\rangle-\langle I\rangle^2$ and the bunching parameter modulus $|b|\equiv|\langle e^{i\theta}\rangle|$ as a function of time, where $\langle\ \rangle$ means average over particles. We recall that the bunching parameter is defined such that $0\leqslant|b|\leqslant 1$ and it assumes its minimum value $|b|=0$ when angles are spread out (θ uniformly distributed along 0 and 2π) and its maximum value $|b|=1$ when they are all the same (completely bunched state).

First we analyze the bunch dynamics as the initial action I_o is varied for a fixed value of the wave amplitude A_w. Results obtained for $A_w=0.5$ and three distinct values of I_o are presented in Fig. 6. Figures 6(a), 6(b), and 6(c) show the time evolutions of $\langle I\rangle$, v_I and $|b|$, respectively. The presence of three different regimes is noted. In the first one, $I_o=10^{-3}$ (solid line), the bunching is actually formed in the very beginning of the dynamics as can be appreciated in Fig. 6(c) and it is maintained throughout the integration period [Fig. 6(b) and 6(c)] during which it keeps revolving along the first island boundary. In this case, particles continuously gain and lose energy from the waves in a quasi-periodic fashion with $\langle I\rangle$ [Fig. 6(a)] presenting peaks of alternating height (as A_w is decreased, these peaks height differences also decrease). Each time that $\langle I\rangle\to 0$, $d_t\theta$ increases greatly and particles spread out, but rapidly bunch again keeping a dynamic of the regular type. The second regime with $I_o=10^{-2}$ (long dashed lines) initially has the same characteristics as the previous one with a bunch formation and an almost periodic bunch-wave interaction. In fact, in the beginning the time evolution of $\langle I\rangle$ is very similar in both cases. However, as time evolves the bunch starts to spread out simultaneously with the onset of particles diffusion, breaking the *regular* acceleration. The interruption of the bunched dynamics takes place because particles are not strictly evolving along the first island boundary, since I_o is nonvanishing. So, unless we are in an ideal case where $I_o=0$, we may always expect an interruption of the bunched dynamics for a given time t_{int}. By this point of view, the two regimes are actually the same, with the only difference that in first one t_{int} was greater than the integration time. Of course, it suffices for an

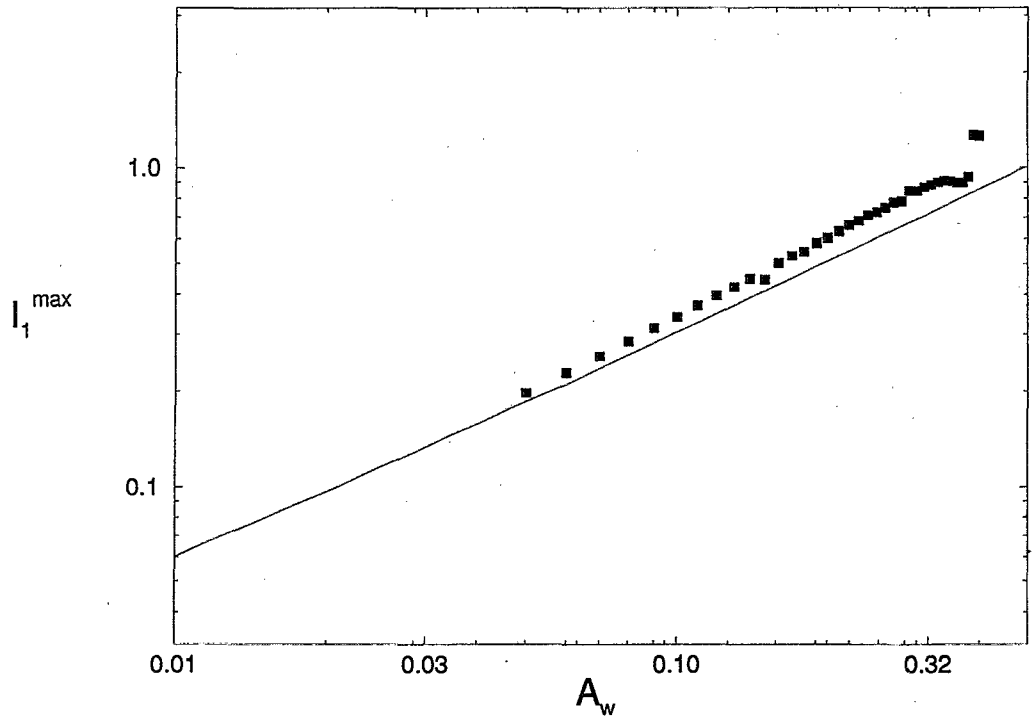

FIG. 8. Maximum action excursion I_{max} vs. the wave amplitude A_w for $k=1$ and $\varepsilon=\varepsilon_{op}$ in a log-log graphic. Squares represent values obtained by numerically integrating particle trajectories and the solid line the ones calculated from Eq. (7).

improved *regular* acceleration that t_{int} is of the order of the period of the bunch-wave interaction. Finally, for $I_o=4\times10^{-1}$ (dashed lines) we find the third regime where no bunching process seems to occur. Particles experience a chaotic diffusion from the beginning of their dynamics in this case.

We now analyze the bunch dynamics as the wave amplitude A_w is varied for a fixed value of the initial action I_o. As before, in Figs. 7(a), 7(b) and 7(c) the time evolutions of $\langle I\rangle$, v_I and $|b|$, respectively, for the case $I_o=10^{-2}$ are shown. Solid lines represent the case $A_w=0.45$ where we identify an initial bunching formation with a quasi-periodic bunch dynamics throughout the integration period. Comparing these results with those presented in Fig. 6 for $A_w=0.5$ and $I_o=10^{-2}$ (long dashed lines) one realizes that as A_w is increased, t_{int} decreases. This behavior is valid until a certain value for the wave amplitude is achieved and above which *regular* acceleration can no longer be attained. Dashed lines in Fig. 7 represents such a case. For $A_w=0.72$ no bunch seems to be formed. Although Fig. 7(c) shows us that an effective bunching occurs for particles angles, Figs. 7(a) and 7(b) proves that particles are, in fact, undergoing a chaotic diffusion process. This value for A_w is in good agreement with the analytical calculations done in the last paragraph of the previous section, which estimated the maximum wave amplitude above which we can no longer attain regular acceleration as $A_{max}\approx0.68$.

The above analysis on bunch dynamics for optimal stationary extraordinary mode amplitude $\varepsilon=\varepsilon_{op}$ can be summarized as follows. For nonideal cases with $I_o\neq0$ regular dynamics will always present a typical interruption time above which bunched dynamics is broken. The interruption time decreases with A_w and increases with I_o. Thus, in order to impose an effective particle acceleration, it is necessary to decrease I_o to compensate interruption effects arriving from growing wave amplitudes. This cannot proceed beyond $A_w=A_{max}$, where regular acceleration is no longer present, even for $I_o=0$.

To conclude the numerical verifications we show in Fig. 8 the maximum action excursion vs. the wave amplitude for the case $\varepsilon=\varepsilon_{op}$, computed by direct integration of the trajectory of an initially low energy particle ($I_o=10^{-2}$). We compare these results with those obtained from Eq. (7) in a log-log graphic. A good agreement is obtained. The disturbances from the monotonical variation in the numerical data are due to bifurcations of secondary chains internal to the first island.[13]

VI. FINAL REMARKS AND SUMMARY

The simulation results presented above indicate that one may really improve particle acceleration by introducing a stationary extraordinary mode in the nonlinear interaction of magnetized particles and perpendicularly propagating electrostatic waves. The presence of smooth longitudinal inhomogeneities in the system (caused, for instance, by inhomogeneities in the background magnetic field) were not taken into account. We believe that the resonance suppression would not be qualitatively modified by the inclusion of such effects, since the formalism is built on the action, which is an adiabatic invariant.

The inclusion of beam-beam interaction in a n-particle formulation (that seems to be more appropriate if one is dealing with not too tenuous beams) would lead to the onset of

Arnold diffusion along the two-dimensional phase-space resonances, affecting the regular acceleration. However, the rate of particle loss due to Arnold diffusion is very small, enabling one to disregard its effect for typical acceleration times.

In conclusion, we have analyzed the effects of introducing a stationary extraordinary mode in the nonlinear interaction of particles and transversal electrostatic waves. It has been found that by suitably choosing the stationary mode amplitude, one is able to suppress the resonance responsible for the chaotization of low energy dynamics. A detailed analysis of the topological effects of the resonance suppression is done. We present analytical estimates of the optimal stationary mode amplitude and the maximum acceleration attained. The main results are tested by numerically integrating particle trajectories.

ACKNOWLEDGMENTS

The authors would like to thank F. B. Rizzato for encouraging and helpful discussions and D. Dillenburg for critical comments.

The work was supported by CNPq and FINEP (Brazil). Numerical analysis was performed on the CRAY YMP-2E at Universidade Federal do Rio Grande do Sul Supercomputing Center.

[1] P. Sprangle, L. Vlahos, and C. M. Tang, IEEE Trans. Nucl. Sci. **NS-30**, 3177 (1983).
[2] C. Chen, Phys. Rev. A **46**, 6654 (1992).
[3] R. Pakter, R. S. Schneider, and F. B. Rizzato, Phys. Rev. E **49**, 1594 (1994).
[4] L. Friedland, Phys. Plasmas **1**, 421 (1994).
[5] S. P. Kuo and M. C. Lee, J. Plasma Phys. **52**, 339 (1994).
[6] R. C. Davidson, Y.-T. Yang and, R. E. Aamodt, J. Plasma Phys. **41**, 405 (1989).
[7] G. Corso and F. B. Rizzato, J. Plasma Phys. **49**, 425 (1993).
[8] D. Farina and R. Pozzoli, Phys. Fluids B **3**, 1570 (1991).
[9] K. Akimoto and H. Karimabadi, Phys. Fluids **31**, 1505 (1988).
[10] A. Fukuyama, H. Momota, R. Itatani, and T. Takizuka, Phys. Rev. Lett. **28**, 701 (1977).
[11] B. V. Chirikov, Phys. Rep. **52**, 263 (1979).
[12] A. J. Lichtenberg and M. A. Lieberman, *Regular and Stochastic Motion* (Springer, New York, 1983).
[13] G. Corso and F. B. Rizzato, Physica D **80**, 296 (1995).
[14] G. Polymilis and K. Hyzanidis, Phys. Rev. E **47**, 4381 (1993).
[15] R. Pakter, G. Corso, T. S. Caetano, D. Dillenburg, and F. B. Rizzato, Phys. Plasmas **1**, 4099 (1994).